Send Orders of Reprints at reprints@benthamscience.org

5414 *Current Medicinal Chemistry,* **2012,** *19,* **5414-5423**

Toxins from *Physalia physalis* (Cnidaria) Raise the Intracellular Ca^{2+} of Beta-Cells and Promote Insulin Secretion

C.M. Diaz-Garcia[1,2], D. Fuentes-Silva[3], C. Sanchez-Soto[1], D. Domínguez-Pérez[4], N. García-Delgado[5], C. Varela[6], G. Mendoza-Hernández[7], A. Rodriguez-Romero[3], O. Castaneda[5] and M. Hiriart*[,1]

[1]Department of Neural Development and Physiology. Instituto de Fisiología Celular. Universidad Nacional Autónoma de México/Circuito Ext. SN, UNAM, Coyoacán, México DF. CP 04510, México; [2]Posgrado en Ciencias Biológicas. Universidad Nacional Autónoma de México; [3]Departamento de Biomacromoléculas. Instituto de Química. Universidad Nacional Autónoma de México; [4]Departamento de Biología, Universidad Central "Marta Abreu" de Las Villas. Carretera a Camajuaní Km 5 1/2, Santa Clara, CP 54830, Cuba; [5]Facultad de Biología. Universidad de La Habana/Calle 25 No. 455, Plaza de la Revolución, La Habana CP 10400, Cuba; [6]Acuario Nacional de Cuba/Ave. 3ra Esq. 62, Playa, La Habana CP 10400, Cuba; [7]Departamento de Bioquímica. Facultad de Medicina. Universidad Nacional Autónoma de México

Abstract: *Physalia physalis* is a marine cnidarian from which high molecular weight toxins with hemolytic and neurotoxic effects have been isolated. In the present work, two novel toxins, PpV9.4 and PpV19.3 were purified from *P. physalis* by bioactive guideline isolation. It involved two steps of column chromatography, gel filtration and RP-HPLC. The molecular weights were 550.7 and 4720.9 Da for PpV9.4 and PpV19.3, respectively. In the light of the Edman sequencing results, the structure of these toxins included the presence of modified amino acids. Both toxins increased the percentage of insulin secreting beta-cells and induced cytosolic Ca^{2+} elevation. To date, this is the first report of low molecular weight toxins increasing insulin secretion purified from cnidarians, by constituting a new approach to the study of beta-cells physiology.

Keywords: Animal experiment, cnidarian venom, cytosolic calcium, glucose tolerance test, insulin release, ion channel, islet beta-cell, mass spectrometry, *Physalia physalis*, toxins.

INTRODUCTION

Physalia physalis [1] belongs to Siphonophores, a group of highly structured colonial organisms [2]. These animals live in a pelagic habitat and they are widely distributed throughout the tropical Atlantic Ocean, with a high population density in the gulf coasts. Its defensive/prey-capturing tentacles present a battery of poisonous stinging cells called nematocytes, which are capable to launch a toxin-containing, harpoon-like structure called nematocyst Fig. (**1**). They present an average diameter from 10.6 to 23.5 µm with the major toxic activity associated to the smaller structures [3].

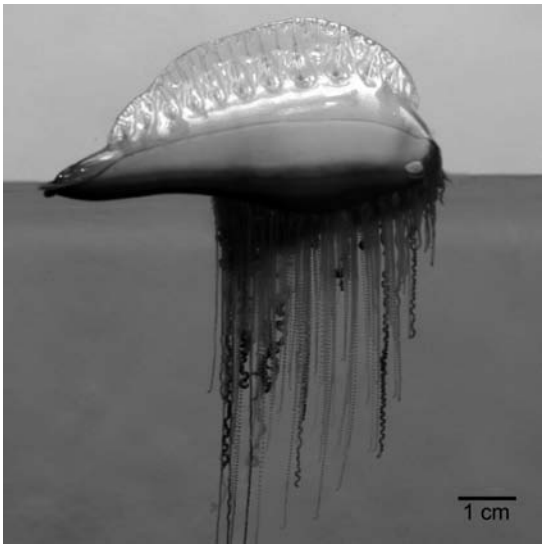

Fig. (1). A colony of *Physalia physalis*. Hanging coiled tentacles are equipped with thousands of nematocysts, containing stinging organelles with a mixture of toxins.

*Address correspondence to this author at the Department of Neural Development and Physiology, Instituto de Fisiología Celular, Universidad Nacional Autónoma de México/Circuito Ext. SN, UNAM, Coyoacán, México DF. CP 04510, México; Tel: 52-55-56225665; Fax: 52-55-56225747; E-mail: mhiriart@ifc.unam.mx

Physalia physalis envenomation has been reported for humans after accidental contact with dactylozooids (defense and prey capture tentacles), that depending on the stinging, can cause a wide range of conditions, from intense pain, nausea, vomiting, linear erythematous plaques and skin necrosis, to systemic symptoms, such as respiratory distress, impaired cardiac activity, and even death [4]. The exocytotic and cytolytic release of histamine from mast cells [5], cutaneous vasopermeability [6], and dilation of the vascular musculature of dogs and rabbits were described among the its biological effects, through a mechanism sensible to antihistamines and prostaglandin synthesis inhibitors [7, 8]. Several cases of man-of-war envenomation develop specific immunoglobulins (Ig), which have been shown to have a cross-reactive immune response with the sea nettle (*Chrysaora quinquecirrha*) toxins [9].

It has also been reported that the *P. physalis* poison increases the Na^+, K^+ and Ca^{2+} transmembranal fluxes in treating embryonic chick heart cells and many cell lines, which cannot be reverted with specific channel blockers [10, 11]. Based on the nonspecific ionic fluxes and the dose-dependent increase in the release of the enzyme lactate dehydrogenase observed in different cell lines [12], the responsible molecule could be a 240 kDa hemolytic protein [13] which represents more than one-fourth of protein content in the nematocyst [14]. Similarly, there are evidences about the neurotoxic effects of high molecular weight compounds in the venom, such as the 85 kDa toxin P_3, that blocks in a reversible and dose-dependent manner the glutamatergic transmission in snail (*Zachrysia guanesis*) neurons and crayfish (*Cambarus clarkii*) neuromuscular junction [15]. Another ion channel modulator is the 200 kDa protein toxin P_1, which exerts an antagonic action against nicotinic cholinergic receptors on snail neurons and frog neuromuscular junction, but not on glutamate receptors. These evidences suggest a complex mechanism involving non-competitive antagonism and channel blockade [16].

To date, to our knowledge, there have been no published reports regarding toxins from *P. physalis* acting on the excitability of pancreatic beta-cells, which secrete insulin and play a major role in glucose homeostasis. The coupling between the elevation of the extracellular glucose concentration and insulin secretion depends on metabolic and ionic mechanisms that can be review elsewhere [17-

1875-533X/12 $58.00+.00

19]. Briefly, the sugar is carried out to beta-cells through passive glucose transporters (GLUT2 in rodents) and metabolized, which in turn increases the ATP/ADP ratio and causes the ATP sensitive K^+ channels blockade. The silencing of the hyperpolarizing K^+ efflux altogether the depolarizing background due to non selective cationic currents, displace the membrane potential to more positive values where significant activation of low voltage activated Ca^{2+} channel (T type) and Na^+ channels occurs. The cationic influx strengthens the depolarization and unfolds the high voltage activated Ca^{2+} channels (L type mainly), which are responsible for Ca^{2+} entry which triggers insulin secretion. In the resulting oscillatory pattern of membrane potential, some voltage and Ca^{2+}-activated K^+ channels contribute to repolarization.

There are many compounds that affect these ion channels and they have been useful to understand the mechanisms underlying insulin secretion [20]. Some of them, for instance, the K^+ channel gating modifiers peptides, have a potential application not only in the study of beta-cell physiology, but also in type 2 diabetes mellitus therapeutics [21]. The bioactive compounds isolated from cnidarians have been useful tools for biomedical research since a long time ago [22] and recently, the presence of low molecular weight compounds that modulate insulin secretion has been demonstrated [23]. However, Cnidaria is still an underexplored taxon, where only a few reports of novel products have been achieved in the class Hydrozoa (where *P. physalis* belongs) during the last decade [24].

In the present work we studied the effects of the crude tentacle-only extract from *Physalia physalis* on insulin secretion of individual native rat beta-cells. Two molecules with insulin secretion-potentiating activities were isolated and a partial biochemical characterization was carried out. These molecules (< 5 kDa) with low molecular weights induce an elevation of the cytosolic Ca^{2+}, as well as insulin secretion, by increasing hormone release by single cells and the recruitment of a secreting subpopulation of beta-cells.

MATERIALS AND METHODS

Sample Collection

Physalia physalis specimens were collected at the coast of La Habana, Cuba. The specimens were brought to the laboratory and kept in clean saline water for the preparation of the crude extract.

Crude Extract Preparation

The crude extract was prepared by modifying a previously described method [25]. Briefly, poisonous tentacles were removed and cut in small pieces. The biological material was homogenized in ice-cold water (1:1 w/v) using a blender, alternating with five to ten periods of 5 seconds of autolysis at room temperature. The crude lysate was clarified through a layer of spun glass and subsequently centrifuged twice at 1145 g for 30 min at 4 ^oC. The supernatant was recovered, lyophilized and stored at -20 ^oC until use.

SDS-PAGE

SDS–PAGE was performed under reducing conditions according to the method of Shagger & von Jagow [26]. The resolving gel contained 16 % polyacrylamide concentration. Proteins and peptides were stained with Coomassie R-250 Brilliant Blue for the determination of their relative molecular weight.

Purification Procedures

Lyophilized crude extract was resuspended in 0.1 M ammonium acetate pH 6.7 to a final concentration of 2.5 mg/ml, and filtered through a 0.22 μm Millipore membrane (Millipore, Billerica, USA). Next, aliquots were subjected to gel filtration on a HiLoad 16/20 Superdex 75 column and their elution diagrams recorded. The column was previously equilibrated and eluted with the sample buffer (0.1 M ammonium acetate buffer pH 6.7) in an Akta FPLC System (GE Healthcare, USA) at a flow rate of 1ml/min. The low molecular weight fractions exhibiting insulin secretion-potentiating activity were pooled and loaded onto a Phenomenex ODS-3 reverse phase column previously equilibrated with 0.1 % aqueous trifluoroacetic acid (TFA). Components were eluted using a linear gradient from 0 % to 100 % of acetonitrile containing 0.12 % TFA, at a flow rate of 1 ml/min. The protein concentration was determined by spectrophotometry using a bicinconinic acid protein assay kit (Thermo Scientific, Rockford, IL. USA) with BSA as standard. Samples were read at 562 nm with a Synergy HT Multi-Mode Microplate Reader (Biotek Instruments, Inc,Vermont, USA).

Purification Table

The insulin secretion-potentiating activity of each purification step was calculated as the fraction of increase in insulin secretion at 5.6 mM (see RHPA section), divided by the volume of assay times the dilution of the toxins. The total activity was then calculated as the potentiating activity times the volume of each purification step, and the specific activity was determined dividing the total activity by the amount of sample from each step. Finally, the percentage of recovery was obtained dividing the total activity of each step by the total activity in the crude extract. Likewise, the purification factor was obtained dividing the specific activity of each purification step by the specific activity of the crude extract.

Mass Spectrometry

Mass spectrometry of the active fraction was performed using a matrix-assisted laser desorption ionization–time of flight MALDI–TOF Omniflex mass spectrometer from Bruker Daltonics (Bremen, Germany) equipped with a pulsed nitrogen laser (λ = 337 nm, 10 ns pulse width). Spectra were acquired in positive-reflection mode with a 19 kV accelerating voltage. The toxins were dissolved in a saturated solution of alpha-ciano-4-hydroxicinnamic acid in 30% acetonitrile, 0.1% trifluoroacetic acid, with Sodium-Trifluoroacetate as a catalyst for ionization. Ribonuclease (14000 Da) and Angiotensin I (1046.2 Da) were used as external standards. The toxin PpV19.3 was sent to Dr. Mary Ann Gawinowicz laboratory to determine its molecular weight at the Protein Core Facility, Columbia University College of Physicians & Surgeons.

N-Terminal Sequencing

The N-terminal sequences of each insulinotropic toxin were determined by Edman degradation using an automatic gas-phase protein sequencer (Model LF 3000, Beckman Instruments, Irvine, USA).

Intraperitoneal Glucose Tolerance Test

Glucose (2 g/kg body weight) was injected intraperitoneally in control (saline) and treated (*P. physalis* crude extract at 0.5, 1 and 4 mg/kg body weight) 8 weeks-old male Wistar rats. Samples were obtained via tail bleeding. Blood glucose levels were measured at 0 (before glucose injection) and 15, 30, 60, 90 and 120 min after glucose administration, using commercial blood glucose meter (Accu-Chek Active, Roche).

Culture of Pancreatic Beta-Cells

All methods used in this study were approved by the Animal Care Committee of the Instituto de Fisiología Celular, Universidad Nacional Autónoma de México. Animal care was performed according to the *"International Guiding Principles for Biomedical Research Involving Animals", Council for International Organizations of Medical Sciences, 2010).* Wistar rats were obtained from

the local animal facility, maintained in a 14:10-h light-dark cycle (0600 – 2000), and allowed free access to standard laboratory rat diet and tap water. On the day of the experiments, animals were anesthetized with intraperitoneal pentobarbital sodium (40 mg/kg), and, after pancreas dissection, animals were euthanized by cervical dislocation.

Pancreatic beta-cells were obtained by adopting the technique previously described [27]. Briefly, pancreatic islets were isolated and separated from the acinar tissue by collagenase digestion and a Ficoll gradient centrifugation; clean islets were then handpicked. Dissociation of the cells was achieved by incubating them in a shaker bath for 10 min at 37°C in calcium-free Spinner solution, with 15.6 mM glucose, 0.5% bovine serum albumin, and 0.01% trypsin, followed by mechanical disruption. Single cells were cultured for 1 day in RPMI-1640 supplemented with 10% fetal calf serum, 200 units/ml penicillin G, 200 mg/ml streptomycin, 0.5 mg/ml amphotericin B and 200 mM L-glutamine.

Reverse Hemolytic Plaque Assay (RHPA)

To identify insulin-secreting cells, RHPA [28] was performed as described previously [29]. Briefly, after 1 day in culture, islet cells were detached from culture dishes, and equal volume of islet cells was mixed with *Staphylococcus aureus* protein A–coated sheep erythrocytes, introduced to Cunningham chambers previously treated with poly-L-lysine to promote cell attachment, and incubated for 1 hour.

Experiments were carried out at 5.6 or 15.6 mM glucose with or without each toxin in the presence of insulin antiserum, and then incubated with guinea pig complement. Insulin released was revealed by the presence of hemolytic plaques around the secreting cells, which result from the complement-mediated lysis of erythrocytes bearing insulin–anti-insulin complexes bound to protein A.

Each coverslip was scanned at a 100X or 400X magnification with a Leika Micro Dissection System 6000 (version 6.4.1.2887) coupled to a Hitachi HV-D20 camera, and the immunoplaque diameters were measured with the aid of the image analyzer software ImageJ from NIH, USA (http:/rsb.info.nih.gov/ij). The plaque size was expressed as area, and the cells that formed plaques were counted. These results were expressed as the percentage of insulin-secreting cells; at least 50 cells were counted per replicate in each experimental condition, in each culture. All experiments were performed at least three times by duplicate.

The effect of the active fraction on the overall glucose-induced secretory activity of beta-cells was also calculated as a secretion index, by multiplying the average immunoplaque area by the percentage of plaque-forming cells [30]. A frequency distribution of immunoplaque areas was constructed with the pooled data from five different experiments by duplicate, to identify functional subpopulations of beta-cells and to determine whether these subpopulations were differentially affected by the experimental treatments. According to the presence of different secreting subpopulations [31], we considered two classifications: small plaque-forming cells (SP: area of immunoplaques $\leq 2000\ \mu m^2$) and large plaque-forming cells (LP: area $> 2000\ \mu m^2$) [32, 33].

Cell Viability

Cell viability was obtained by Trypan blue exclusion assay. Briefly, 25 000 cells were plated in 96 well microplates and incubated with 200 µl of supplemented RPMI 1640 medium during 8 hours. Media was replaced by an equivalent solution to that used in the RHPA, by adding 50 µl of control or treatment-containing HBSS medium to each well. Finally 0.4 % of HBSS-diluted (1:10) Trypan blue solution was added and after 3 min, blue-stained cells (dead cells) and bright living cells were counted. At least 100 cells from three random fields were analyzed and the percentage of living cells was calculated by dividing the number of living cells by the total number of counted cells.

Cytosolic Ca^{2+} Measurement

Cells were plated in glass coverslips coated with 0.5 mg/ml Poly-L-lysine. After 24 - 48 hours of culture, cells were loaded during 30 min with 1 µM of Ca^{2+} indicator Fluo-4AM (Molecular Probes) in Hanks Balanced Salt Solution supplemented with 200 units/ml penicillin G, 200 mg/ml streptomycin and 0.1 % BSA, washed with the same medium (3 volumes) and allowed to equilibrate for 20 min. Beta-cells were viewed through a 60x oil immersion objective and fluorescence was measured with a 488 nm excitation and 535 nm emission using a BioRad MRC 1024 microscope and the Confocal Assistant version 4.02 software. Images were acquired every 3.5 seconds for 10 minutes at 17°C. Sequence files were analyzed using the image analyzer software ImageJ from NIH, USA (http:/rsb.info.nih.gov/ij). Regions of interest were selected on the cells and the average pixel intensity was measured. The percentages of fluorescence changes ($\Delta F/F_o$) were plotted as a function of time. Adjusting the exponential decay of each signal without stimulation and subtracting the curve to the recordings corrected loss of fluorescence due to photo bleaching.

Data Analysis

Comparisons were performed by a *t-student* test using GraphPad InStat version 3.00 (GraphPad Software, San Diego California USA, www.graphpad.com). Paired *t-student* tests were performed for RHPA experiments. Graphics were constructed using Origin version 7 (OriginLab Corporation, Northampton USA, www.OriginLab.com).

RESULTS

2.1. SDS-PAGE Analysis of Crude Extract

Lyophilized crude extract of *P. physalis* (Pp_{ce}) was dissolved in 20 mM Tris-HCl pH 8.0 and then analyzed by denaturing and reducing SDS-PAGE. Staining with Coomassie Brilliant Blue R-250 revealed a complex mixture with high and low molecular weight components Fig. (**2**) that could be divided into three zones. A high-molecular-weight zone from 200 to 55 kDa in which two intense staining bands at 66 and 55 kDa were observed. A second zone containing middle molecular weight bands corresponded to 40-25 kDa, where three closely bands migrated between 25 and 30 kDa. The third zone corresponded to the low molecular weight components, which were not well resolved in the gel and migrated as a broad and diffuse band in the range of 10 to 6 kD.

Further crude extract was used to perform an intraperitoneal glucose tolerance test (IPGTT) and a Reverse Hemolytic Plaque Assay (RHPA) to measure its effect on insulin release of single primary rat beta-cells.

2.2. *Physalia physalis* Crude Extract Lowers Blood Glucose Levels *in Vivo*

P. physalis crude extract (Pp_{ce}) was tested in an IPGTT at three non lethal doses of 0.5, 1 and 4 mg/kg. We observed a dose-dependent lowering effect of Pp_{ce} on blood glucose levels, which resulted in a significant 28% reduction of the area under the curve when rats were inoculated with 4 mg/kg of Pp_{ce} Fig. (**3**). The reducing activity of the venom on plasma glucose levels could be interpreted as an increased insulin secretion by pancreatic beta-cells and/or a higher sensitivity of target organs to the hormone. Recently, we have reported that an active fraction from *Z. sociatus* that impairs insulin release also causes glucose intolerance [23]. Therefore, we tested if the reduction of the area under the curves in the

IPGTT of Pp_{ce} treated rats could reflect an increased insulin secretion of pancreatic beta-cells, measured by a RHPA.

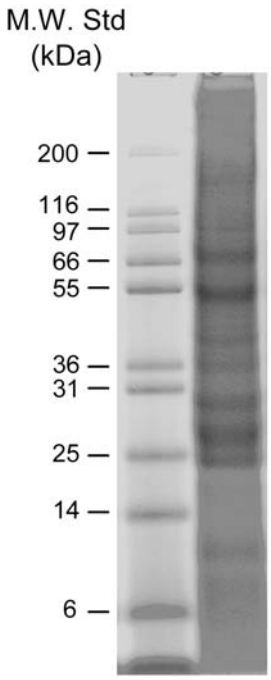

Fig. (2). SDS-PAGE profile of the soluble proteins of *P. physalis* crude extract on a 16 % gel. Molecular weights of standard proteins are listed to the left of the gel.

2.3. Bioassay-Guided Purification of *Physalia physalis* Toxins

The crude extract solution was subjected to evaluation of the insulin-secretion activity on individual native rat beta-cells through a RHPA. Isolated beta-cells were incubated at 5.6 and 15.6 mM of extracellular glucose, which resemble basal and elevated glucose levels, respectively. The last mentioned to evaluate the glucose-induced insulin secretion process. *P. physalis* crude extract (500 µg/ml) augmented immunoplaque areas around secreting cells in both conditions, with an increment of 80 % in insulin secretion at 5.6 mM Fig. (**4**). The glucose-independent effect of the crude extract could account for the significant reduction ($p < 0.05$) of blood glucose levels at 90 and 120 min of the IPGTT curve, respect to fasting level in the 4 mg/kg treated rats. This effect can be compared to certain medicinal plants with hipoglycemic effects that increase insulin secretion at 5.6 mM glucose in an insulin-secreting cell line [34].

In order to isolate the active molecule(s) of the *P. physalis* crude extract, a bioassay-guided purification protocol was performed, which involved two steps of column chromatography, gel filtration and reversed-phase high-performance liquid chromatography (RP-HPLC). Six A280 nm peak fractions, PpI, PpII, PpIII, PpIV, PpV and PpVI, were obtained through elution with 0.1 M ammonium acetate buffer pH 6.7 using gel filtration on Superdex 75 Fig. (**5A**). Each fraction was analyzed for insulin secretion activity. The activity was recovered in the low molecular weight fraction PpV, which exhibited a 1.76-fold increase of immunoplaque areas at basal glucose and a significant 1.18-fold increase at 15.6 mM glucose, when applied at a concentration of 300 µg/ml Fig. (**5B**). These effects were similar to those observed for Pp_{ce} at a higher concentration.

The active PpV fractions were pooled and subjected to RP-HPLC on C18 column for further purification. One major peak and four minor peaks were obtained Fig. (**6**). The major peak was eluted with the retention time of 9.4 min and had a weak activity; while one minor peak that eluted at 19.3 min exhibited a potent activity at the same concentration. (Table **1**) shows the purification parameters of the two toxins. The overall level of recovery obtained for *P. physalis* toxins was of 3 % and 12 % for PpV9.4 and PpV19.3, respectively. Both, the purification factor and the level of recovery can be considered as high, if compared with other cnidarians toxins purified by gel filtration and RP-HPLC procedures [35].

2.4. Toxins from *P. physalis* Increase the Overall Insulin Release by Enhancing the Average Secretion and Recruiting a Subpopulation of Secreting Beta-Cells

PpV9.4 did not induce a significant increase in immunoplaque areas at 60 µg/ml (1447 ± 74 μm^2 v.s 1331 ± 59 μm^2 of controls, n = 3, each by duplicate), but caused a two-fold increase when applied at 130 µg/ml in an external solution containing 5.6 mM of glucose. The toxin PpV19.3 reached a similar level of activity at 60 µg/ml. Both toxins also augmented the fraction of secreting beta-cells, which resulted in a 2.4 and a 2.1-fold increases for PpV9.4 and PpV19.3, respectively, in the secretion index, a measure of the overall insulin secretion (Table **2**).

From the analysis of secreting beta-cells subpopulations at 5.6 mM glucose, the recruitment of a new fraction of secreting cells by

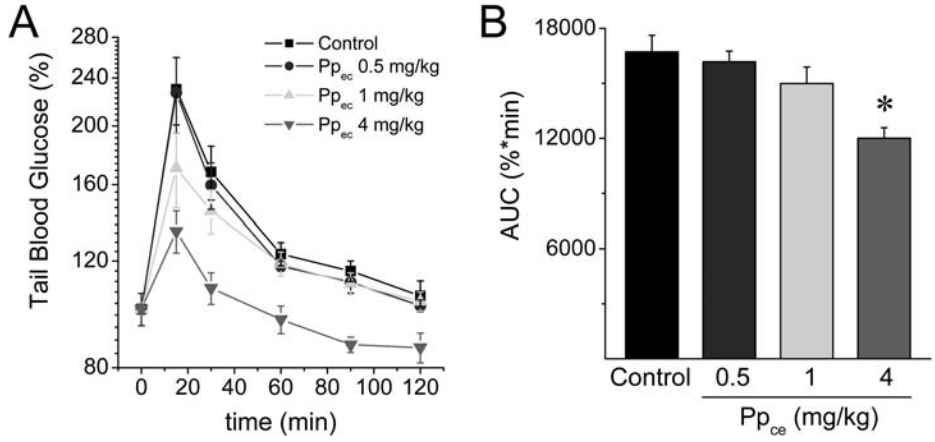

Fig. (3). Intraperitoneal glucose tolerance test. (a) Tolerance curves of Control (n = 7) and *P. physalias* crude extract treated rats (Pp_{ce}) at doses of 0.5 (n = 4), 1 (n = 7) and 4 mg/kg (n = 3) show a marked reduction of glucose levels in Pp_{ce} treated rats at the maximal dose. **(b)** Comparison of the areas under the curves (AUC) in each condition. At the maximal dose, Pp_{ce} significantly reduced the AUC with a * $p < 0.05$. Control blood glucose level = 104 ± 10 mg/dl.

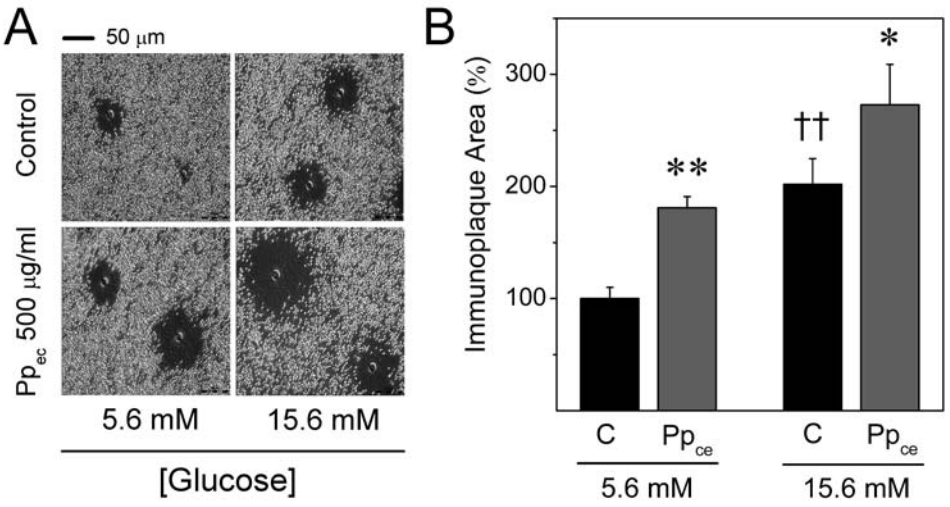

Fig. (4). ***P. physalis*** **crude extract increases insulin secretion of pancreatic beta-cells. (A)** Representative photomicrographs of insulin Immunoplaque Areas (IPA) measured by a Reverse Hemolytic Plaque Assay (RHPA), in each specified condition. Scale bar 50 μm. **(B)** Comparison among Control (**C**) and Pp_{ce} (500 μg/ml) treated cells shows a significant increase in IPA at both glucose concentrations. IPA values are represented by bars, mean ± SEM of 3 different experiments by duplicate, where at least 50 cells were measured per chamber. IPAs are the dark regions around beta cells, which were formed by one hour incubation of islet cells in 5.6 mM or 15.6 mM glucose, in the presence of an insulin antibody and complement. Immunoplaque areas are directly proportional to the insulin secreted by the isolated cells. * $p < 0.05$, ** $p < 0.01$ for comparison between control and Pp_{ce} at the same glucose concentration. †† $p < 0.01$ for comparison between controls of different glucose concentrations. Control IPA at 5.6 mM = 1897 ± 192 μm^2.

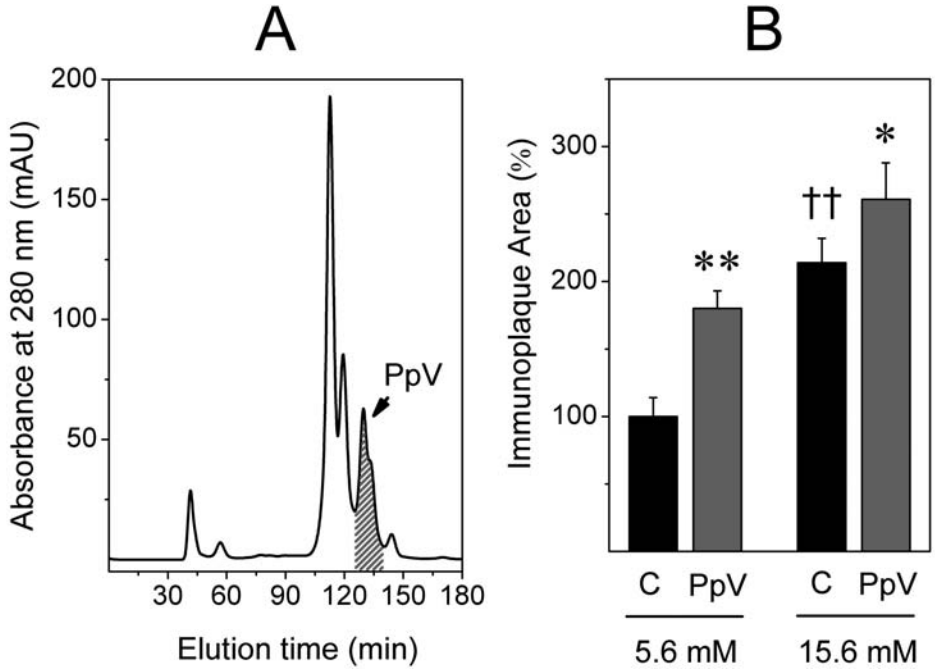

Fig. (5). A low molecular weight fraction from *P. physalis* crude extract potentiates insulin secretion of pancreatic beta-cells. (**A**) The chromatogram at 280 nm, obtained by gel filtration, shows a shaded region that represents the pooled fraction where the potentiating activity upon insulin secretion was recovered. (**B**) Incubation with 300 μg/ml of the active fraction (PpV) caused an increment of IPA. Bars represent mean ± SEM of 3 different experiments by duplicate, where at least 50 cells were measured per chamber. * $p < 0.05$, ** $p < 0.01$ for comparison between control and PpV at the same glucose concentration. †† $p < 0.01$ for comparison between controls of different glucose concentrations. Control IPA at 5.6 mM = 1769 ± 247 μm^2.

the treatments with both toxins, is accompanied by a displacement of the secreting behavior of individual cells from a low rate (fraction of SP cells) to a higher degree of hormone release (LP cells). At 15.6 mM the potentiating effect relays on an increment of IPA without altering the total percentage of secreting cells Fig. (**7**). However, in the 130 μg/ml PpV9.4 condition, there is a significant shift from SP to LP cells.

2.5. Low Molecular Weight Toxins from *P. physalis* Raise the Intracellular Ca^{2+}

The potentiating effect of the low molecular weight fraction PpV on basal secretion could not be related to the main targets of cnidarians neurotoxins: the voltage dependent ion channels [36], which significantly contribute to Ca^{+2} influx and exocytosis in beta-cells at high glucose [17]. We explored if the active toxins could

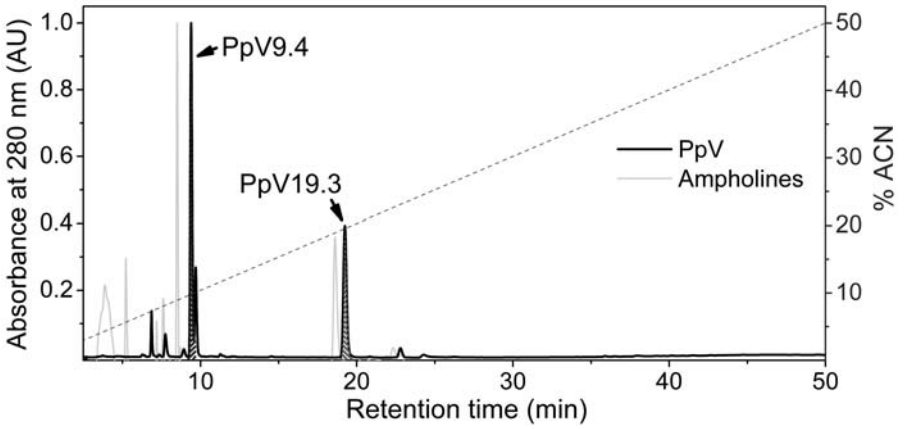

Fig. (6). RP-HPLC Chromatograms of the active fraction PpV. Shaded peaks from the chromatogram at 280 nm correspond to molecules that resembled the potentiating effect on insulin secretion of isolated beta-cells. The toxins were named according to their retention times. PpV9.4 and PpV19.3 eluted within the retention times of a mixture of molecules structurally related to acylpolyamines.

Table 1. Scheme of Purification of the PpV9.4 and PpV19.3 Toxins from *P. physalis*

	Yield					
Fraction Name	**Volume (ml)**	**Sample (mg)**	**Total Activity (U/ml)**	**Specific Activity (U/mg)**	**Recovery* (%)**	**Purification Factor* (Fold)**
Crude extract Pp_{ce}	80	207	92800	448	100	1
PpV	720	83	69840	841	75	1.9
PpV9.4	308	1.6	2772	1733	3	3.9
PpV19.3	881	3.1	11453	3695	12	8.2

*Recoveries are expressed as the percentage of initial Total activity, and Purification factors are calculated on the basis of Specific activities.

Table 2. Toxins from *P. physalis* Potentiate the Overall Insulin Secretion by Increasing the Amount of Hormone Release and the Fraction of Secreting Cells

	IPA* (μm²)		F*		SI* (μm²)	
	5.6 mM	**15.6 mM**	**5.6 mM**	**15.6 mM**	**5.6 mM**	**15.6 mM**
Control	1704 ± 116	2903 ± 231††	0.35 ± 0.01	0.49 ± 0.01††	587 ± 37	1420 ± 119††
PpV9.4	2807 ± 242**	3449 ± 212*	0.49 ± 0.02**	0.51 ± 0.03	1413 ± 207**	1766 ± 133*
PpV19.3	2795 ± 184**	3547 ± 429*	0.43 ± 0.02**	0.53 ± 0.03	1218 ± 130**	1913 ± 275*

* Toxins Pp9.4 and Pp19.3 caused a similar potentiating effect on Immunoplaque Areas (IPA) and the total Fraction of secreting cells (F) when applied at 130 μg/ml and 60 μg/ml respectively. The combined effects are analyzed through the Secretion Index (SI).

raise the intracellular Ca^{+2} of beta-cells at 5.6 mM glucose, in the presence of 100 nM tetrodotoxin (TTX), 300 μM $NiCl_2$, 10 μM nifedipine and 100 nM ω-conotoxin GVIA which block Na^+ and type T, L and N voltage gated Ca^{+2} channels, respectively. Under these conditions, PpV9.4 (130 μg/ml) caused an immediate increment in Ca^{+2} oscillations, while PpV19.3 (60 μg/ml) rise the intracellular Ca^{+2} approximately 2 min after application Fig. (**8A**). The areas under the curves were integrated from the application of vehicle or toxin to the end of the 10 min recordings, which constituted a measure of the amount of Ca^{+2} ions entering the cells. Both toxins statistically increased the area under the Ca^{+2}–sensitive fluorescence curves Fig. (**8B**), which coincides with the increment in the basal insulin secretion.

2.6. Biochemical Characterization of PpV9.4 and PpV19.3 Toxins

2.6.1. Mass Spectrometry Analysis

The MALDI mass spectrum of the PpV9.4 toxin showed an intense peak that appeared at *m/z* 550.7 Da, together with two less abundant peaks (Supplemental Fig. **1**). The last fact is probably due to the presence of small amounts of the peak eluting on RP-HPLC, closely to the PpV9.4 toxin. The molecular weight of this toxin falls within the range of other bioactive compounds from the phylum, such as diterpenoids [37, 38], sesquiterpenoids [39], biscembranoids [40] and steroids [41]. Like the molecules mentioned before, PpV9.4 could be a small molecule that share hidrophobic and hydrophilic properties according to its retention time in the C18 RP-HPLC chromatogram. Thereby, it appears possible that PpV9.4 may consist of a small organic molecule or in another case to be a very short peptide. Small molecules from natural sources have a great potential in the field of drug discovery [42], especially for treating diabetes.

In contrast, the mass spectra of the second purified PpV19.3 toxin included a single peak at *m/z* 4720.19 Da (Supplementary Fig. **1**). This signal matched with the typical molecular weight range of the cnidarians peptide toxins whose masses are comprised between 3 and 7 kDa [43, 44].

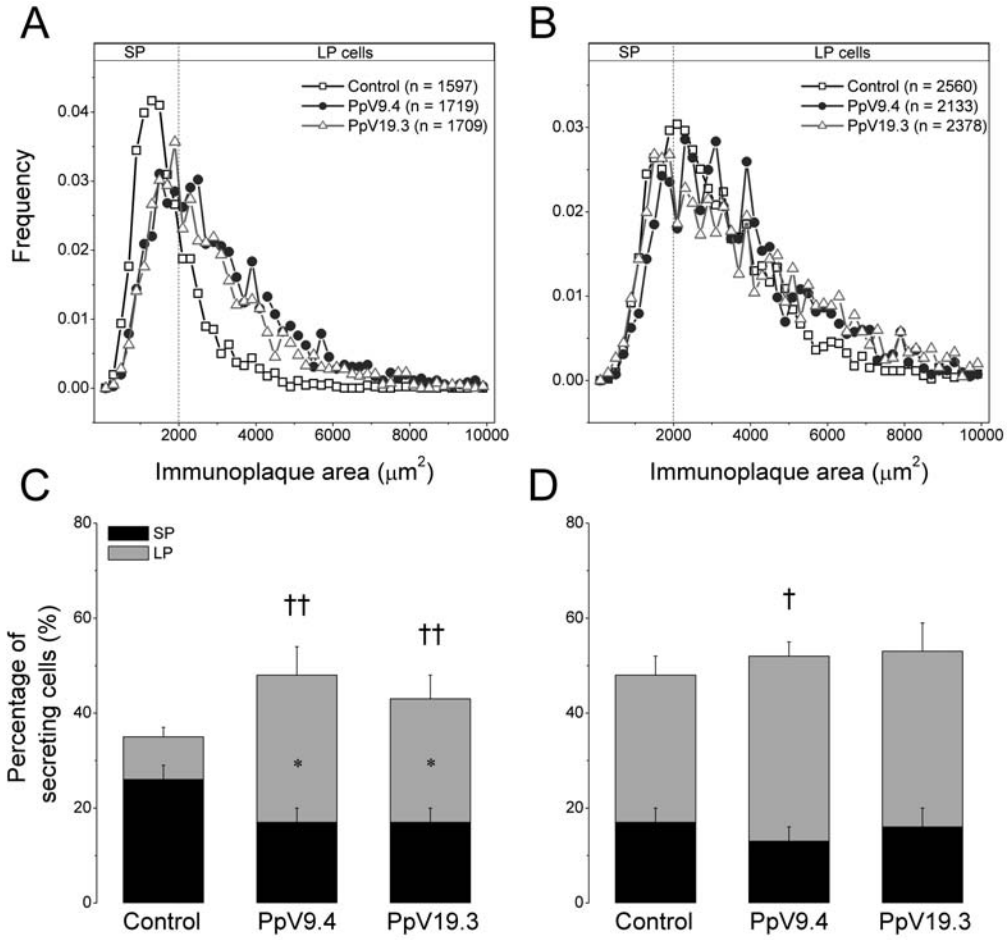

Fig. (7). Active toxins from fraction PpV increase the percentage of secreting cells. (a, b) Histograms of Immunoplaque Areas of Control and toxin treated cells incubated at 5.6 mM and 15.6 mM glucose, respectively. Frequencies were calculated by counting the number of IPAs in 250 μm^2 intervals from 0 to 10000 μm^2, and dividing it by the total number of cells. The cutoff value at 2000 μm^2 separate two distinguishable, but overlapping secreting populations of beta-cells, the small plaque (SP) and the large plaque (LP) forming plaque cells. **(c, d)** Percentage of SP and LP secreting cells in control and toxins treated cells at basal and high glucose respectively. Values are represented by bars, mean ± SEM of 5 different experiments by duplicate, where at least 150 cells were measured per chamber. The tested concentration for PpV9.4 and PpV19.3 toxins were 130 and 60 μg/ml, respectively. * $p < 0.05$ for comparison between control and treated cells SP subpopulations; $^{\dagger}p < 0.05$ and $^{\dagger\dagger}p < 0.01$ for comparison of LP subpopulation in the same conditions.

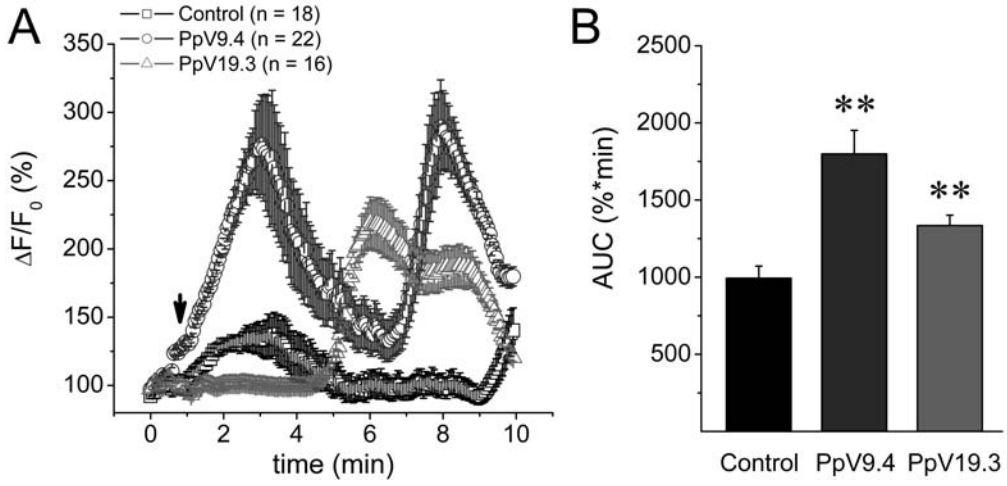

Fig. (8). ***P. physalis*** **toxins enhance insulin secretion by increasing the intracellular Ca^{2+} of pancreatic beta-cells. (a)** Average traces of relative changes in Ca^{2+} sensitive fluorescence of control and toxin treated cells incubated at 5.6 mM glucose. Arrow indicates the application of PpV9.4 (130 μg/ml) or Pp19.3 (60 μg/ml) to the bath solution. **(b)** Comparison of areas under the curves (AUC) from traces of Ca^{2+} imaging experiments show higher rises of intracellular Ca^{2+} from toxin treated cells. Bars represent mean ± SEM. ** $p < 0.01$ for comparison between control and toxin treated cells.

2.6.2. Edman Degradation and Analysis of the HCl Hydrolysis

In order to demonstrate the peptide nature of the PpV19.3 toxin and to obtain any structural information of PpV9.4 toxin, we used the automatic Edman degradation procedure to identify N-terminal residues in both toxins. As result, the analysis of the purified PpV9.4 toxin revealed one major peak eluting at a retention time of 8.62 min, near the appropriate retention time as is determined to phenylthiohydantoin (PTH)-asparagine, though the definite identification of this residue was not possible. Indeed, it is conceivable idea that this signal belongs to a new modified amino acid. On the contrary, another eluted peak identified in the sequence of PpV9.4 matched with PTH-tryptophan. In contrast, Edman degradation of PpV19.3 toxin revealed in the first two cycles the presence of PTH-tyrosine, -leucine and –tryptophan, in addition to the similar peak at 8.88 unidentified in PpV9.4 and a peak that eluted at 12.33 min, which was not matched with any PTH-residue standard. Therefore, these results strongly suggest that PpV19.3 could be a new class of marine toxin containing amino acid in its structure and showing a molecular weight characteristic of peptide toxins.

On the other hand, PpV9.4 present features consistent with the reported for acylpolyamines. The results of the amino acid sequencing for each toxin are shown in (Supplementary Fig. **2**). Four cycles of Edman degradation were performed on each toxin and there was no activity observed in the third cycle of the degradation, which indicated that only two and five residues are contained into the PpV9.4 and PpV19.3 respectively. Insulin pattern was submitted to analysis by Edman degradation as control of the sequencing protein for quality assurance of our sequences determined. The sequence analysis confirmed the first four N-terminal amino acid residues of both chain A (GIVE) and chain B (FVNQ).

To corroborate the presence of the residues identified by Edman degradation in the structures of PpV9.4 and PpV19.3, the toxin samples were exhaustively hydrolyzed with HCl (3N) at 37 ^{o}C during 8 hours and then hydrolysates were analyzed by C18 RP-HPLC. Chromatogram profiles were compared with those recorded for trytophan and tyrosine standards. As shown in (Supplementary Fig. **3**), several products were released from PpV19.3 toxin, which exhibited a complex profile when compared to PpV9.4. In the hydrolysate of PpV19.3 the presence of tryptophan and tyrosine was detected, which was accordant with the result obtained by Edman degradation. However, a simple chromatography elution profile was achieved in the hydrolysate of PpV9.4, where only two major peaks were observed and any peak could not be identified with tryptophan or asparagine probably because during HCl hydrolysis asparagine is converted to aspartic acid and tryptophan is oxidized.

DISCUSSION

Polyamine-containing toxins are ubiquitous polycationic molecules at physiological pH that modulate a variety of ionotropic receptors. They have been identified by RP-HPLC with a C18 column as the low molecular weight compounds eluting, in a linear gradient of ACN from 0 % to 60 % (v/v), between 10 and 30 min [45]. In this concern, the comparison of the retention times between the two toxins isolated from *P. physalis* and a mixture of organic molecules structurally related to acylpolyamines, at the same chromatographic conditions, shows that both toxins elute within the range of acylpolyamines. This chromatographic behavior might suggest similarities in the molecular nature of the toxins PpV9.4 and PpV19.3. Interestingly, acylpolyamines commonly occur in spider venoms and constitute a group of polar compounds usually with molecular weights below 1 kDa, that modulate ionotropic glutamate receptors as well as other neuronal ion channels [46, 47]. However, in recent years a collection of unusually long-chain polyamines (LCPAs), as well as a new family of small peptides that are post-translationally modified by the attachment of long-chain polyamines have been isolated from the marine sponge, *Axinyssa aculeate* [48, 49]. Latest is a recent example of a novel structural feature reported for naturally occurring peptides from marine organism, which is a reach source of unusual compounds showing unexpected interactions with mammalian cells.

The ability of both toxins to elevate the cytosolic Ca^{2+} when most of the voltage gated ion channels were blocked, rise many questions about their mechanisms of action. So far, it is not likely that they act in a similar fashion; instead, we can speculate that the fast effect of PpV9.4 seems to be directly on some TRP channel or glutamate ionotropic receptor, which are permeable to Ca^{2+} and functionally relevant to insulin secreting cells [50, 51].

Interestingly, Cuypers and coworkers (2006) [52] found a sensitizing activity on the vanilloid member 1 of the Transient Receptor Potential family of ion channels (TRPV1) in a similar crude extract from *Physalia physalis*, and associated with the resulting increment in the currents with a persistent burning-pain sensation. TRPV1 is a Ca^{2+}-permeable ion channel that has been related to insulin secretion [17, 50]. It is clear that this channel is present in the sensorial fibers that innervate the pancreatic islets and participate in the modulation of insulin secretion, as well as insulin resistance and islet inflammation [53]. The presence of functional TRPV1 channels have been demonstrated in the rat insulinoma INS-1E cell line [54] and certain studies indicate that they are also present in native beta-cells, although it is still a controversial issue [55]. Several TRP channels are involved in insulin secretion, contributing to the early depolarization and also to the membrane voltage and intracellular Ca^{2+} oscillations of beta-cells [56]. These channels could be a potential target for cnidarians toxins increasing insulin secretion.

The increment of intracellular Ca^{2+} by PpV19.3, is delayed with respect to that of PpV9.4 and possibly related to slower processes, such as metabotropic receptors or G protein mediated signaling cascades which are present in beta-cells and regulate Ca^{2+} release from intracellular stores [57, 58]. It is clear that the enhanced insulin release is not a collateral effect of cytotoxicity, since none of the toxins, or the crude extract, caused a significant change in cell viability (Supplementary Fig. **4**). The unraveling of the full structure and the exact mechanisms of action of both toxins is a matter of further research.

It is known that the venom from *Physalia physalis* tentacles possesses great similarity with that of the hydra, considering their high molecular weight cytolytic toxins composition and biological effects [13, 59]. However, it has also been proposed that the hydra lacks of the classical Na^{+} and K^{+} channel peptide neurotoxins of sea anemones [59, 60].

In the present study we have purified and characterized two novel low molecular weight toxins from *Physalia physalis* tentacle-only crude extract. The purified toxins have been designated according to their retention times as PpV9.4 and PpV19.3. N-terminal sequencing by Edman degradation revealed that both toxins contain amino acids found in acylpolyamines, as well as signals unidentified, which may suggest the presence of modified amino acids with new structural features, as was recently reported to *A. aculeate* [49]. For this reason, currently structural studies using the combination of MS/MS and NMR experiments are being carried out to know the two *P.physalyis* toxins structures described in this work, which may represent a valuable issue in the field of the structural toxinology. In contrast, until now only cytochrome oxidase subunit-I [61], voltage-gated potassium channel (GenBank: ABD59027.1) and the beta subunit of the calcium channel (GenBank: ABD59026.1) [62], three high molecular weight proteins, are the only ones that have been reported for this specie. Therefore, this is the first report, to our knowledge, of low molecular weight toxins obtained from this specie.

The isolated *P. physalys* toxins potentiate insulin secretion by increasing the cytosolic Ca^{2+} concentration. The exact mechanism

by which the toxins raise the intracellular Ca^{2+} is currently studied. It may be possible that some ion channels and/or signaling cascades could be affected not only in beta-cells but also in other excitable tissues, broadening the biological activities of such toxins. The anti-diabetic potential of bioactive compounds from marine sources, such as algae-derived polysaccharydes with stimulatory activities on insulin secretion of RIN-5F cells, is the focus of intense research [63]. Then, the discovery of novel bioactive compounds from *P. physalis* with potentiating activity on the beta-cells at basal glucose constitutes a first approximation to obtain new approaches in the study of beta-cells physiology and it may constitute a tool for the treatment of insulin related disorders.

Our work has been conducted in beta-cells isolated from non-diabetic normoglycemic rats, which at 15.6 mM glucose almost saturate the response of insulin secretion, measured by the RHPA [30, 64]. We have not assayed the possible effect of PpV9.4 or PpV19.3 on diabetic conditions. However, in this condition the response of beta cells to glucose is altered.

The effectiveness of the toxins in pathological conditions is an interesting question that should be explored in future work, along with a pharmacological analysis of them (i.e. dose-response curves). However, it is known that for certain drugs which potentiate insulin secretion, such as blockers of K_{ATP} channels; their potency varies according to the dose and the glucose levels [65]. Some of them are completely ineffective at maximal stimulating glucose concentrations [66].

CONCLUSIONS

In conclusion, the present work shows that poisonous tentacles of *Physalia physalis* contain low molecular weight compounds with different chemical nature, which affect beta-cells excitability mainly at basal glucose, increasing the intracellular Ca^{2+} without a direct activation of voltage-gated channels.

CONFLICT OF INTEREST

The author(s) confirm that this article content has no conflicts of interest.

ACKNOWLEDGEMENTS

The authors are grateful to Dr. Mary Ann Gawinowicz for mass determination of PpV19.3 toxin. To Ana María Escalante Gonzalbo, Francisco Pérez Eugenio and Efrén A. Robledo, from the Computer Unit to Dr. Aracely and Félix Sierra, for excellent technical support. All from the Instituto de Fisiología Celular, Universidad Nacional Autónoma de México (UNAM). Also to Acela Pedroso from Instituto de Endocrinología de Cuba for liophylization and photographer Rafael Mesa for *P. physalis* picture. To A.S. Gandini for art work. Work in the laboratory of M. Hiriart is supported by Gobierno del Distrito Federal PICDS08-72, CONACYT CB2009-131647, and DGAPA-PAPIIT IN215611, Universidad Nacional Autónoma de México. C.M. Diaz-Garcia is the recipient of a Doctoral Fellowship (CVU/Becario: 356396/245301) from Consejo Nacional de Ciencia y Tecnología (CONACyT).

REFERENCES

[1] Linnaeus, C., **1758**, *Tomus I*, 1-824.
[2] Dunn, C. *Curr Biol*, **2009**, *19*, R233-4.
[3] Burnett, J. W.; Ordonez, J. V.; Calton, G. J. *Toxicon*, **1986**, *24*, 514-8.
[4] Haddad, V., Jr.; da Silveira, F. L.; Cardoso, J. L.; Morandini, A. C. *Toxicon*, **2002**, *40*, 1445-50.
[5] Cormier, S. M. *J Exp Zool*, **1984**, *231*, 1-10.
[6] Burnett, J. W.; Calton, G. J. *Toxicon*, **1986**, *24*, 614-7.
[7] Loredo, J. S.; Gonzalez, R. R., Jr.; Hessinger, D. A. *J Pharmacol Exp Ther*, **1985**, *232*, 301-4.
[8] Loredo, J. S.; Gonzalez, R. R., Jr.; Hessinger, D. A. *J Pharmacol Exp Ther*, **1986**, *236*, 140-3.
[9] Russo, A. J.; Calton, G. J.; Burnett, J. W. *Toxicon*, **1983**, *21*, 475-80.
[10] Larsen, J. B.; Lane, C. E. *Comp Biochem Physiol*, **1970**, *34*, 333-8.
[11] Edwards, L.; Luo, E.; Hall, R.; Gonzalez, R. R., Jr.; Hessinger, D. A. *Toxicon*, **2000**, *38*, 323-35.
[12] Edwards, L.; Hessinger, D. A. *Toxicon*, **2000**, *38*, 1015-28.
[13] Tamkun, M. M.; Hessinger, D. A. *Biochim Biophys Acta*, **1981**, *667*, 87-98.
[14] Burnett, J. W.; Calton, G. J. *Toxicon*, **1987**, *25*, 581-602.
[15] Mas, R.; Menendez, R.; Garateix, A.; Garcia, M.; Chavez, M. *Neuroscience*, **1989**, *33*, 269-73.
[16] Menendez, R.; Mas, R.; Garateix, A.; Garcia, M.; Chavez, M. *Comp Biochem Physiol C*, **1990**, *95*, 63-9.
[17] Hiriart, M.; Aguilar-Bryan, L. *Am J Physiol Endocrinol Metab*, **2008**, *295*, E1298-306.
[18] Ashcroft, F. M.; Rorsman, P. *Prog Biophys Mol Biol*, **1989**, *54*, 87-143.
[19] Henquin, J. C.; Meissner, H. P. *Experientia*, **1984**, *40*, 1043-52.
[20] Diaz-Garcia, C. M.; Sanchez-Soto, C.; Hiriart, M. *Cell Mol Neurobiol*, **2010**, *30*, 1275-81.
[21] Herrington, J. *Toxicon*, **2007**, *49*, 231-8.
[22] Suput, D. *Toxicon*, **2009**, *54*, 1190-200.
[23] Diaz-Garcia, C. M.; Sanchez-Soto, C.; Fuentes-Silva, D.; Leon-Pinzon, C.; Dominguez-Perez, D.; Varela, C.; Rodriguez-Romero, A.; Castaneda, O.; Hiriart, M. *Toxicon*, **2012**, *59*, 306-14.
[24] Rocha, J.; Peixe, L.; Gomes, N. C.; Calado, R. *Mar Drugs*, **2011**, *9*, 1860-86.
[25] Gómez, T.; Romero, D. L.; Wong, L.; Barral, A. M.; Martínez, J. R.; Chávez, M. A. *Rev. Cubana Invest. Biom.*, **1986**, *5*, 117-125.
[26] Schagger, H.; von Jagow, G. *Anal Biochem*, **1987**, *166*, 368-79.
[27] Diaz-Villasenor, A.; Sanchez-Soto, M. C.; Cebrian, M. E.; Ostrosky-Wegman, P.; Hiriart, M. *Toxicol Appl Pharmacol*, **2006**, *214*, 30-4.
[28] Neill, J. D.; Frawley, L. S. *Endocrinology*, **1983**, *112*, 1135-7.
[29] Aguayo-Mazzucato, C.; Sanchez-Soto, C.; Godinez-Puig, V.; Gutierrez-Ospina, G.; Hiriart, M. *PLoS One*, **2006**, *1*, e35.
[30] Hiriart, M.; Ramirez-Medeles, M. C. *Endocrinology*, **1991**, *128*, 3193-8.
[31] Hiriart, M.; Ramirez-Medeles, M. C. *Mol Cell Endocrinol*, **1993**, *93*, 63-9.
[32] Sanchez-Soto, M. C.; Larrieta, M. E.; Vidaltamayo, R.; Hiriart, M. *Diabetologia*, **1999**, *42*, 1086-92.
[33] Rosenbaum, T.; Sanchez-Soto, M. C.; Hiriart, M. *Diabetes*, **2001**, *50*, 1755-62.
[34] Hussain, Z.; Waheed, A.; Qureshi, R. A.; Burdi, D. K.; Verspohl, E. J.; Khan, N.; Hasan, M. *Phytother Res*, **2004**, *18*, 73-7.
[35] Uechi, G.; Toma, H.; Arakawa, T.; Sato, Y. *Protein J*, **2011**, *30*, 422-8.
[36] Honma, T.; Shiomi, K. *Mar Biotechnol (NY)*, **2006**, *8*, 1-10.
[37] Chen, B. W.; Chao, C. H.; Su, J. H.; Wen, Z. H.; Sung, P. J.; Sheu, J. H. *Org Biomol Chem*, **2010**, *8*, 2363-6.
[38] Chen, Y. H.; Tai, C. Y.; Su, Y. D.; Chang, Y. C.; Lu, M. C.; Weng, C. F.; Su, J. H.; Hwang, T. L.; Wu, Y. C.; Sung, P. J. *Mar Drugs*, **2011**, *9*, 934-43.
[39] Su, J. H.; Chiang, M. Y.; Wen, Z. H.; Dai, C. F.; Hsu, C. H.; Sheu, J. H. *Chem Pharm Bull (Tokyo)*, **2010**, *58*, 250-3.
[40] Yan, P.; Deng, Z.; van Ofwegen, L.; Proksch, P.; Lin, W. *Mar Drugs*, **2010**, *8*, 2837-48.
[41] Chai, X. Y.; Sun, J. F.; Tang, L. Y.; Yang, X. W.; Li, Y. Q.; Huang, H.; Zhou, X. F.; Yang, B.; Liu, Y. *Chem Pharm Bull (Tokyo)*, **2010**, *58*, 1391-4.
[42] Liu, Q.; Chen, L.; Hu, L.; Guo, Y.; Shen, X. *Biochim Biophys Acta*, **2010**, *1799*, 854-65.
[43] Castaneda, O.; Harvey, A. L. *Toxicon*, **2009**, *54*, 1119-24.
[44] Moran, Y.; Gordon, D.; Gurevitz, M. *Toxicon*, **2009**, *54*, 1089-101.
[45] Moore, S.; Smyth, W. F.; Gault, V. A.; O'Kane, E.; McClean, S. *Rapid Commun Mass Spectrom*, **2009**, *23*, 1747-55.
[46] Estrada, G.; Villegas, E.; Corzo, G. *Nat Prod Rep*, **2007**, *24*, 145-61.
[47] Scott, R. H.; Sutton, K. G.; Dolphin, A. C. *Trends Neurosci*, **1993**, *16*, 153-60.
[48] Sufrin, J. R.; Finckbeiner, S.; Oliver, C. M. *Mar Drugs*, **2009**, *7*, 401-34.
[49] Matsunaga, S.; Jimbo, M.; Gill, M. B.; Wyhe, L. L.; Murata, M.; Nonomura, K.; Swanson, G. T.; Sakai, R. *Chembiochem*, **2011**, *12*, 2191-200.
[50] Uchida, K.; Tominaga, M. *Endocr J*, **2011**.
[51] Inagaki, N.; Kuromi, H.; Gonoi, T.; Okamoto, Y.; Ishida, H.; Seino, Y.; Kaneko, T.; Iwanaga, T.; Seino, S. *FASEB J*, **1995**, *9*, 686-91.
[52] Cuypers, E.; Yanagihara, A.; Karlsson, E.; Tytgat, J. *FEBS Lett*, **2006**, *580*, 5728-32.
[53] Razavi, R.; Chan, Y.; Afifiyan, F. N.; Liu, X. J.; Wan, X.; Yantha, J.; Tsui, H.; Tang, L.; Tsai, S.; Santamaria, P.; Driver, J. P.; Serreze, D.; Salter, M. W.; Dosch, H. M. *Cell*, **2006**, *127*, 1123-35.
[54] Jabin Fagelskiold, A.; Kannisto, K.; Bostrom, A.; Hadrovic, B.; Farre, C.; Eweida, M.; Wester, K.; Islam, M. S. *Islets*, **2012**, *4*.
[55] Islam, M. S. *Adv Exp Med Biol*, **2011**, *704*, 811-30.
[56] Colsoul, B.; Vennekens, R.; Nilius, B. *Rev Physiol Biochem Pharmacol*, **2011**, *161*, 87-110.
[57] Cline, G. W.; Zhao, X.; Jakowski, A. B.; Soeller, W. C.; Treadway, J. L. *Biochem Biophys Res Commun*, **2011**, *412*, 413-8.
[58] Oya, M.; Suzuki, H.; Watanabe, Y.; Sato, M.; Tsuboi, T. *Genes Cells*, **2011**, *16*, 608-16.
[59] Sher, D.; Zlotkin, E. *Toxicon*, **2009**, *54*, 1148-61.
[60] Oliveira, J. S.; Redaelli, E.; Zaharenko, A. J.; Cassulini, R. R.; Konno, K.; Pimenta, D. C.; Freitas, J. C.; Clare, J. J.; Wanke, E. *J Biol Chem*, **2004**, *279*, 33323-35.

[61] Ortman, B. D.; Bucklin, A.; Pages, F.; Youngbluth, M. *Deep-Sea Research II*, **2010**, *57*, 2148-2156.
[62] Bouchard, C.; Price, R. B.; Moneypenny, C. G.; Thompson, L. F.; Zillhardt, M.; Stalheim, L.; Anderson, P. A. *J Exp Biol*, **2006**, *209*, 2979-89.
[63] Zhang, D.; Fujii, I.; Lin, C.; Ito, K.; Guan, H.; Zhao, J.; Shinohara, M.; Matsukura, M. *Biol Pharm Bull*, **2008**, *31*, 921-4.
[64] Hiriart, M.; Martinez, M. T.; Ramirez-Medeles, M. C. *Adv Exp Med Biol*, **1997**, *426*, 267-74.
[65] Fuhlendorff, J.; Rorsman, P.; Kofod, H.; Brand, C. L.; Rolin, B.; MacKay, P.; Shymko, R.; Carr, R. D. *Diabetes*, **1998**, *47*, 345-51.
[66] Joost, H. G.; Hasselblatt, A. *Naunyn Schmiedebergs Arch Pharmacol*, **1979**, *306*, 185-8.

Received: March 16, 2012 **Revised: July 04, 2012** **Accepted: July 19, 2012**